

## RESEARCH ARTICLE

View Article Online  
View Journal | View IssueCite this: *Org. Chem. Front.*, 2022, **9**, 633

## Vinyl sulfonyl chemistry-driven unidirectional transport of a macrocycle through a [2]rotaxane†

Arthur H. G. David, Pablo García-Cerezo, Araceli G. Campaña, Francisco Santoyo-González \* and Victor Blanco \*

By applying a combination of the coupling-and-decoupling (CAD) chemistry of the vinyl sulfonate group with the click thia-Michael addition to the vinyl sulfone group (MAVS) we performed the irreversible unidirectional transportation of the ring through the linear component in a [2]rotaxane by a chemically and pH-driven flashing energy ratchet mechanism. The design is based on a monostoppered thread precursor bearing a sulfonate stopper, a vinyl sulfone group on the unstoppered end and a dibenzylammonium unit as recognition site for the dibenzo-24-crown-8 macrocycle. First, the ring enters from the vinyl sulfone side and the rotaxane is capped through a thia-Michael addition reaction. Then, the cleavage of the sulfonate group of the opposite stopper using  $MgBr_2$  as chemical stimulus and subsequent addition of base ( $Et_3N$ ) promoted the controlled and directional release of the macrocycle into the bulk under mild conditions. The efficiency of the system allowed the *in situ* operation as demonstrated by NMR and HRMS techniques.

Received 5th October 2021,  
Accepted 25th November 2021

DOI: 10.1039/d1qo01491a

rsc.li/frontiers-organic

## Introduction

The main reason for the importance and relevance of mechanically interlocked molecules (MIMs),<sup>1</sup> such as rotaxanes<sup>2</sup> and catenanes,<sup>3</sup> is probably their use to design, prepare and operate artificial molecular machines in an attempt to mimic nature or to perform a certain task.<sup>4</sup> Typically, molecular machines built on the basis of MIMs rely on molecular switches in which the position of the macrocycle can be controlled through the use of external stimuli. For rotaxanes, the translational motion of the macrocycle along its axle induced by these stimuli gave rise to the preparation of nanovalves,<sup>5</sup> the production of macroscopic work,<sup>6</sup> the modulation of photophysical properties,<sup>7</sup> and to applications in switchable catalysis<sup>8</sup> or molecular electronics.<sup>9</sup> Moreover, the rotaxane architecture also enabled the generation of synthesizers,<sup>10</sup> elevators<sup>11</sup> or muscles.<sup>12</sup>

The development of directional transport systems using interlocked structures is one of the most significant progress in the field of molecular machines since it allows an operation away from the equilibrium, a crucial element for the development of molecular motors or pumps.<sup>13</sup> Indeed, the key feature

of these synthetic devices is the unidirectional movement of a component of the system respect to another. This net transport is produced following Brownian ratchet mechanisms<sup>14</sup> and is generally controlled by photo-switches,<sup>15</sup> redox processes,<sup>16</sup> or chemical fuels.<sup>17</sup>

Recently, cleavable rotaxanes<sup>18</sup> started to attract attention and arose as an interesting alternative to induce a net transport of the macrocycle along the axle. Thus, Chen and co-workers reported the unidirectional transportation of a ring in a rotaxane architecture by performing a CuAAC reaction on one side of a mono-stoppered thread in a pseudorotaxane as the capping step of the process, followed by a selective DBU-catalyzed elimination on the vicinity of a triazolium group on the other side of the rotaxane as a stopper cleavage reaction (decoupling step) that enabled the release of the macrocycle.<sup>19</sup> Later on, they proposed another design based on the use of fluoride to release the wheel by cleavage of a *tert*-butyldiphenylsilyl group.<sup>20</sup> More recently, Stoddart and co-workers have applied the same concept of stopper cleavage, in this case light-triggered, to release the macrocycle from a molecular pump.<sup>21</sup>

On the other hand, the click Michael-type addition reaction of nucleophiles to vinyl sulfonyl groups (MAVS),<sup>22</sup> such as vinyl sulfone or vinyl sulfonate, is an efficient and versatile tool for the synthesis of rotaxanes, as we recently demonstrated.<sup>23</sup> Furthermore, the vinyl sulfonate moiety is an appropriate group for coupling-and-decoupling chemistry (CAD),<sup>24</sup> since after the MAVS, it can undergo substitution by nucleophiles under relatively mild conditions.<sup>25</sup> Thus, we demonstrated the utility of this CAD chemistry both to build a rotaxane and to subsequently chemically cleave it in a controlled manner to

Departamento de Química Orgánica, Facultad de Ciencias, Unidad de Excelencia de Química Aplicada a Biomedicina y Medioambiente (UEQ), Universidad de Granada (UGR), Avda. Fuente Nueva S/N, 18071 Granada, Spain. E-mail: jsantoyo@ugr.es, victorblancos@ugr.es

† Electronic supplementary information (ESI) available: Experimental procedures, characterization data, NMR and HRMS spectra and additional supporting figures. See DOI: 10.1039/d1qo01491a



disassemble it into its components, thus, allowing the development of a cleavable rotaxane.<sup>23</sup>

Therefore, we envisaged that the chemistry of vinyl sulfone and vinyl sulfonate groups could be an efficient tool for the development of rotaxanes that could enable the pH- and chemically-controlled unidirectional transport of the ring through the linear component. In this context, here we report an irreversible unidirectional transportation system of a macrocycle based on a [2]rotaxane architecture that relies on both the MAVS and the vinyl sulfonate CAD chemistry.

## Results and discussion

### Strategy and system design

The proposed operation for the unidirectional macrocycle transport is based on a flashing energy ratchet mechanism employing chemical and acid/base stimuli. For this purpose we designed a monostoppered axle precursor bearing a vinyl sulfone group on one end while on the other a sulfonate stopper was previously introduced through a thia-Michael addition to a vinyl sulfonate moiety. The system also incorporates a dibenzylammonium unit as binding site for the dibenzo-24-crown-8 (DB24C8) macrocycle ( $K_a = 2.7 \times 10^4 \text{ M}^{-1}$  in  $\text{CDCl}_3$ ).<sup>26</sup> The operation would start with the pseudorotaxane assembly under thermodynamic control driven by the establishment of hydrogen bond interactions between the ammonium unit and the macrocycle followed by the rotaxane formation *via* a capping approach through a MAVS reaction to the vinyl sulfone unit. Nucleophilic displacement of the sulfonate group to cleave the corresponding sulfonate-functionalized stopper group and addition of base to deprotonate the amine and remove the hydrogen bond interactions with the macrocycle would lead to the release of the macrocycle through the opposite side of its entrance, thus, achieving the unidirectional transport of the macrocycle (Fig. 1).

During this operation, the establishment of a pseudorotaxane would represent a lower energy situation than the free axle

and macrocycle and, therefore, it would be energetically favoured. Although the complexation is an equilibrium process, the relatively high binding constant along with the appropriate experimental conditions would allow a high degree of complexation. In this process, the bulky stopper would constitute an unsurmountable energy barrier, thus, the ring would be threaded through the vinyl sulfone side. After the subsequent capping and formation of the [2]rotaxane, the potential energy barrier of the vinyl sulfone side would increase, avoiding the disassembly of the system. The subsequent decoupling of the sulfonate moiety would cause a decrease of the potential energy barrier on that side, while the addition of base would imply a destabilization of the resulting pseudorotaxane as the hydrogen bonding interactions are no longer present and complexation cannot occur. As result, the macrocycle would be released into the bulk towards a lower energy status, completing its unidirectional path (Fig. 1).

### Synthesis, operation and characterization

The synthetic route towards our system started with the preparation of aldehyde **6** (Scheme 1). Williamson reaction between 4-hydroxybenzaldehyde (**1**) and 3-bromo-1-propanol, followed by a protection of the aldehyde group as an acetal employing 2,2-dimethyl-1,3-propanediol afforded intermediate **2** in good yield (85% and 73% for the first and second step, respectively). Treatment with 2-chloroethanesulfonyl chloride in basic medium gave vinyl sulfonate **3** in 80% yield. Subsequent MAVS reaction with thiol stopper **4**<sup>23</sup> yielded compound **5** in excellent yield (quant). Finally, cleavage of the acetal moiety with trifluoroacetic acid afforded aldehyde **6** in 95% yield.

To obtain the target thread precursor we performed a reductive amination between aldehyde **6** and amine **7** (see the ESI† for its synthesis) followed by a Boc-protection of the resulting dibenzylamine derivative giving intermediate **8** in very good yield (80%). Finally, treatment with  $\text{CF}_3\text{CO}_2\text{H}$  and  $\text{Et}_3\text{SiH}$  cleaved both trityl and Boc protecting groups. Subsequent reprotection of the amine followed by a MAVS reaction

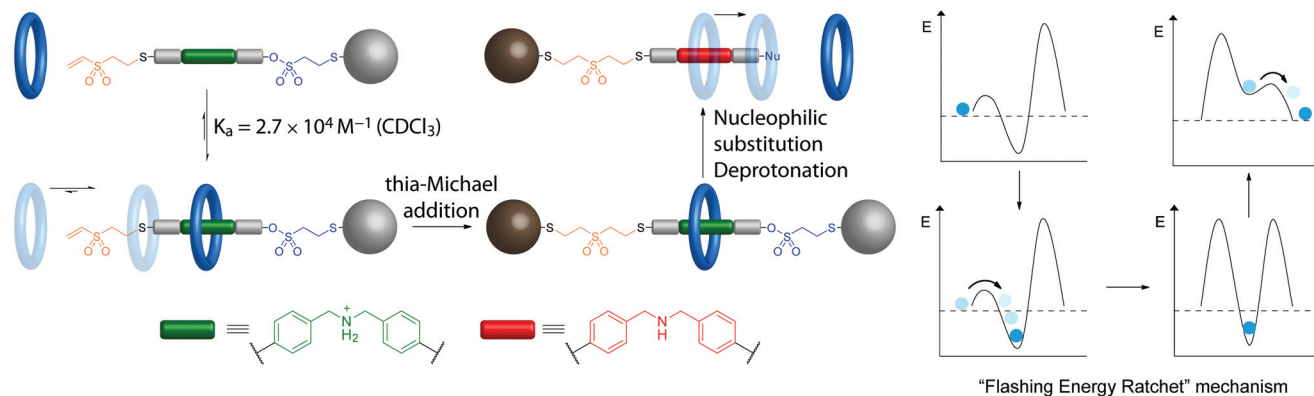
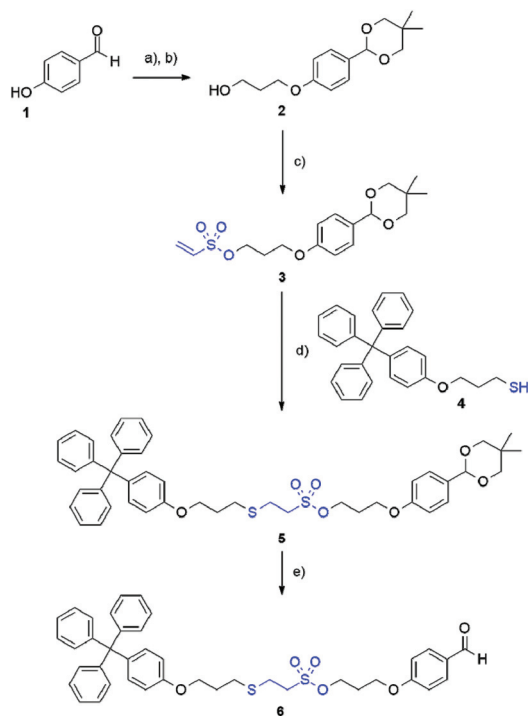


**Fig. 1** Proposed strategy for the unidirectional and irreversible transportation of a macrocycle through the linear element of a [2]rotaxane following a flashing energy ratchet mechanism and exploiting the reactivity of the vinyl sulfone and vinyl sulfonate groups. The binding constant between DB24C8 and the dibenzylammonium motif in  $\text{CDCl}_3$  has been taken from ref. 26.

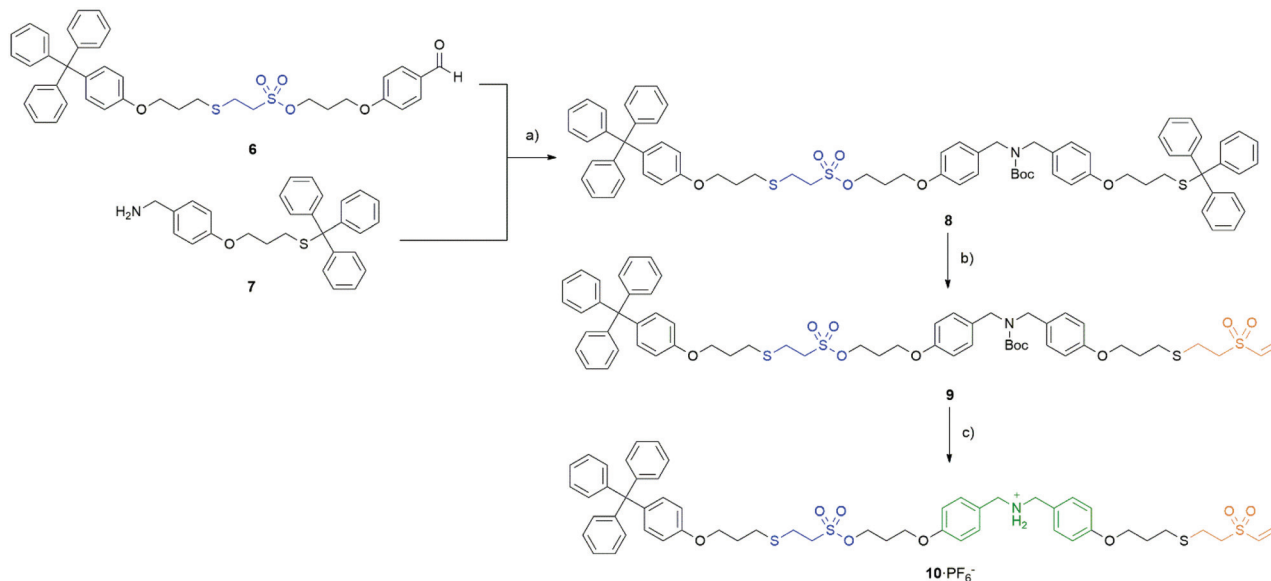




**Scheme 1** Synthesis of aldehyde **6**: reagents and conditions: (a) 3-Bromo-1-propanol,  $K_2CO_3$ ,  $CH_3CN$ ,  $75\text{ }^\circ\text{C}$ , 24 h, 85%. (b) 2,2-dimethyl-1,3-propanediol,  $DL$ -10-camphorsulfonic acid, molecular sieves (3 Å), toluene,  $100\text{ }^\circ\text{C}$ , 18 h, 73%. (c) 2-chloroethanesulfonyl chloride,  $Et_3N$ ,  $CH_2Cl_2$ ,  $0-4\text{ }^\circ\text{C}$ , 1 h, 80%. (d)  $Et_3N$ ,  $PPh_3$ ,  $CH_2Cl_2/PrOH$  (8 : 1), r.t., 24 h, quant. (e)  $CF_3CO_2H$ ,  $H_2O$ ,  $CH_2Cl_2$ , r.t., 5 h, 95%.

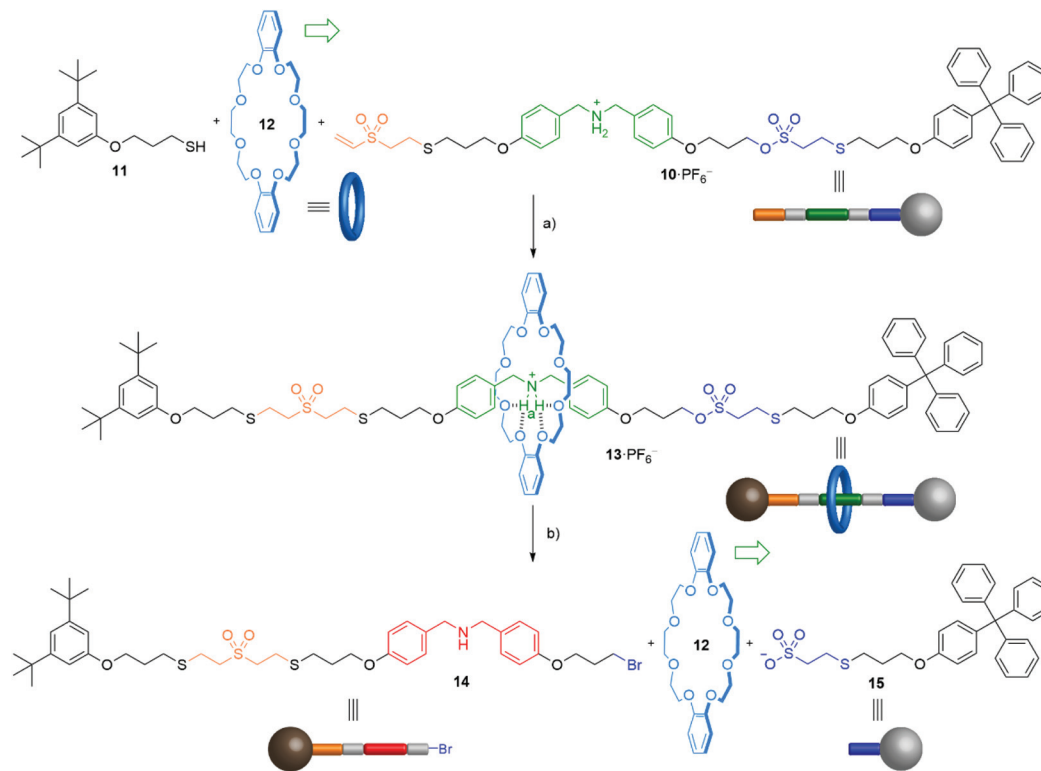
between the resulting thiol and divinyl sulfone afforded **9**. A final deprotection of the amine, followed by protonation and counterion exchange, afforded the thread precursor  $10\text{-PF}_6^-$  in an overall 44% yield (from **8**) (Scheme 2).

Having synthesized the thread precursor  $10\text{-PF}_6^-$ , we carried out the synthesis of free thread  $S12\text{-PF}_6^-$  (see ESI†) as reference for the  $^1H$  NMR analysis and to test the thia-Michael addition reaction, which afforded good results. Then, we started the stepwise transportation of macrocycle **12** through the linear component, tackling the synthesis of rotaxane  $13\text{-PF}_6^-$ . Therefore, we carried out the supramolecular assembly of the pseudorotaxane composed by  $10\text{-PF}_6^-$  and DB24C8 (**12**). This threading is an equilibrium process, being the complexation between macrocycle and dibenzylammonium derivate favoured by the moderately high binding constant in  $CDCl_3$ , which ensures a good degree of association at NMR concentrations. However, to further displace the equilibrium towards the pseudorotaxane and maximize the extent of complexation, higher concentrations (0.021 M or higher for  $10\text{-PF}_6^-$ ) and an excess of DB24C8 (5 equiv.) were used (see Experimental section in the ESI†).  $^1H$  NMR analysis showed, once equilibrium was reached, two set of signals, one for the pseudorotaxane and a second one for the excess of macrocycle. In this sense, the right integration of the diagnostic NMR signals (see below) and the fact that no free  $10\text{-PF}_6^-$  was detected (e.g. no signals for uncomplexed Hd and He were observed), supported a high degree of association (Fig. S1 and S2†). Subsequently we performed a DMAP-catalyzed MAVS reaction<sup>23,28</sup> of thiol stopper **11** (see ESI† for the synthesis) to the terminal vinyl sulfone group in  $10\text{-PF}_6^-$  at  $0\text{ }^\circ\text{C}$ , yielding the target [2]rotaxane  $13\text{-PF}_6^-$  in 66% yield (Scheme 3a).



**Scheme 2** Synthesis of thread precursor  $10\text{-PF}_6^-$ : reagents and conditions: (a) 1.  $MeOH/THF$  (8 : 5), r.t., 24 h; 2.  $NaBH_4$ ,  $MeOH/THF$  (8 : 5), r.t., 24 h; 3.  $Boc_2O$ ,  $Et_3N$ ,  $CH_2Cl_2$ , r.t., 24 h, 80%. (b) 1.  $CF_3CO_2H$ ,  $Et_3SiH$ ,  $CH_2Cl_2$ , r.t., 6 h; 2.  $Boc_2O$ ,  $Et_3N$ ,  $CH_2Cl_2$ , r.t., 5 h; 3. divinyl sulfone,  $Et_3N$ ,  $CH_2Cl_2$ , r.t., 14 h, 52% (over 3 steps). (c) 1.  $CF_3CO_2H$ ,  $CH_2Cl_2$ , r.t., 5 h; 2.  $HCl$  (2 M in  $Et_2O$ ),  $CH_2Cl_2$ , r.t., 3 h; 3.  $KPF_6$ ,  $CH_2Cl_2/acetone/H_2O$  (4 : 5 : 5), r.t., 18 h, 84% (over 3 steps).





**Scheme 3** Unidirectional transport of DB24C8 (12) through the formation and cleavage of rotaxane **13**·PF<sub>6</sub><sup>-</sup>: reagents and conditions: (a) DMAP<sub>(cat)</sub>, CHCl<sub>3</sub>, 0 °C, 72 h, 66%. (b) 1. MgBr<sub>2</sub>, CHCl<sub>3</sub>, r.t., 48 h; 2. Et<sub>3</sub>N, CDCl<sub>3</sub>, r.t., 10 min, 92% (for 12) and 70% (for 14/15 (1 : 1)).

[2]rotaxane **13**·PF<sub>6</sub><sup>-</sup> was characterized by means of 1D and 2D NMR techniques. As it can be seen on the comparison of its <sup>1</sup>H NMR spectrum with those of the free thread and macrocycle, the aromatic hydrogen nuclei on both rotaxane components suffered some changes (Fig. 2). Thus, the signals of the crown ether aromatic H atoms (H4 and H5) no longer showed the same chemical shift observed in the spectrum of the free macrocycle in CDCl<sub>3</sub> as a result of a more pronounced difference in the chemical environment of those nuclei, while those from the axle suffer an upfield shift. Regarding the CH<sub>2</sub> signals, the benzylic protons from the thread show the typical downfield shift ( $\Delta\delta_{\text{Hb,Hc}} = 0.53$  ppm) associated with the establishment of hydrogen bonds between the ammonium unit and the macrocycle, meanwhile those from the ring are shielded ( $\Delta\delta_{\text{H1}} = -0.40$  ppm;  $\Delta\delta_{\text{H2}} = -0.17$  ppm;  $\Delta\delta_{\text{H3}} = -0.03$  ppm). These variations in the <sup>1</sup>H NMR spectrum are typical for this type of recognition motif based on hydrogen bonding, supporting the formation of the interlocked rotaxane architecture. Furthermore, the ammonium H atoms also exhibit an upfield shift ( $\Delta\delta_{\text{Ha}} = -1.03$  ppm), because of their interaction with the crown ether macrocycle (Fig. 2). Moreover, the DOSY NMR spectrum of **13**·PF<sub>6</sub><sup>-</sup> exhibits the signals from the both the ring and the axle diffusing at the same diffusion coefficient (Fig. 3a).

To further confirm the interlocked nature of **13**·PF<sub>6</sub><sup>-</sup> we also recorded and analyzed the NMR spectrum of the isolated compound in DMSO-*d*<sub>6</sub>. DMSO is a hydrogen bond acceptor, so its

strong competitive character in hydrogen bonding interactions precludes any binding between macrocycle and dibenzylammonium motifs in non-interlocked species.<sup>26</sup> In this case, we could observe changes in the chemical shift of the signals of the dibenzylammonium unit and that of macrocycle H1 that follow the same trends already seen and discussed in CDCl<sub>3</sub> (Fig. S3<sup>†</sup>). Moreover, the DOSY experiment in DMSO-*d*<sub>6</sub> also shows that the structure diffuses as a whole, with the signals corresponding to the macrocycle and the thread showing the same diffusion coefficient (Fig. S4<sup>†</sup>).

Lastly, analysis by ESI-TOF high-resolution mass spectrometry confirmed the identity of [2]rotaxane **13**·PF<sub>6</sub><sup>-</sup>. Indeed, the spectrum shows a signal corresponding to an ion resulting from the loss of the PF<sub>6</sub><sup>-</sup> counterion with an exact mass ( $m/z = 1708.7335$ ) and isotopic distribution that nicely match the theoretical ones (Fig. 3b).

The next step was the cleavage of [2]rotaxane **13**·PF<sub>6</sub><sup>-</sup> exploiting the CAD chemistry of the vinyl sulfonate group. For this purpose, we ideally wanted to find a nucleophilic substitution proceeding without the need of a base, at room temperature and in a chlorinated solvent. After a few unsuccessful attempts, we rediscovered a reaction described by Gore and co-workers in 1976,<sup>29</sup> which was scarcely employed since then. Thus, MgBr<sub>2</sub> was capable of displacing sulfonate groups in CH<sub>2</sub>Cl<sub>2</sub> or CHCl<sub>3</sub> at room temperature in a near quantitative fashion, creating bromoalkanes. Therefore, after successfully testing this reaction with thread **S11** (see ESI<sup>†</sup>) we applied it to



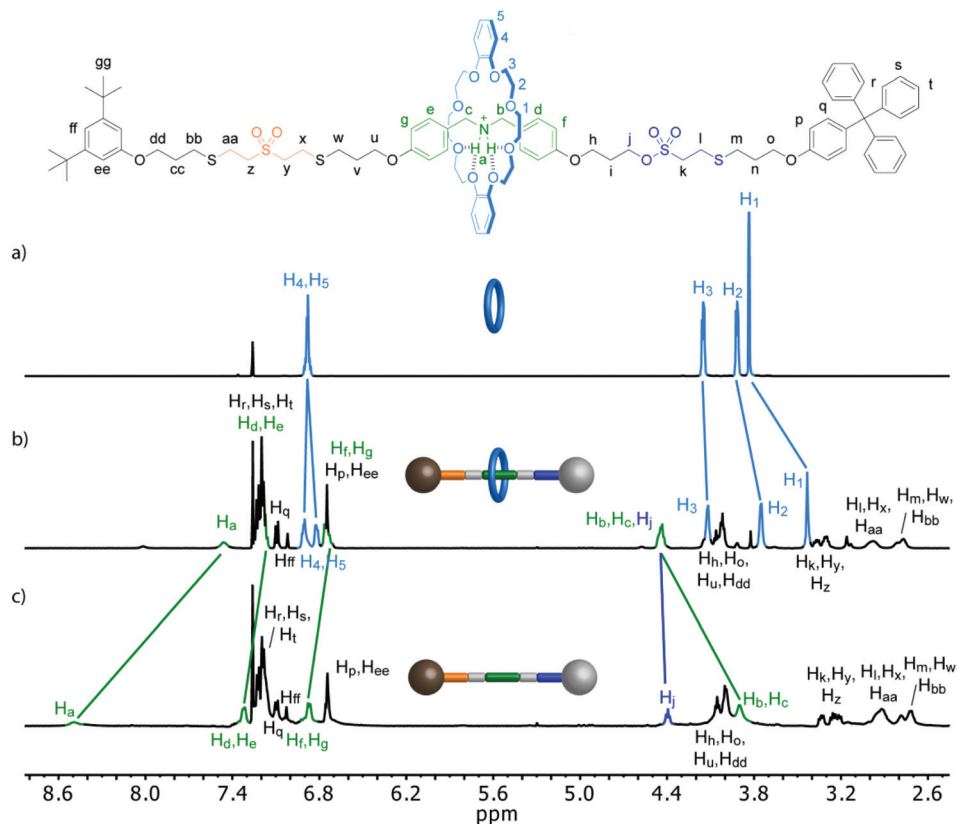


Fig. 2  $^1\text{H}$  NMR (500 MHz,  $\text{CDCl}_3$ ) spectra of: (a) Macrocycle **12**. (b) Rotaxane **13**· $\text{PF}_6^-$ . (c) Thread **S12**· $\text{PF}_6^-$ .

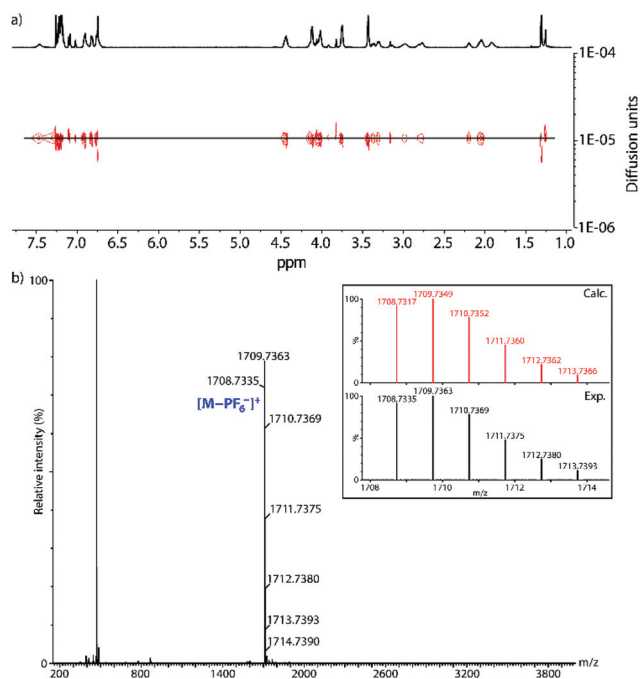


Fig. 3 (a) DOSY NMR (500 MHz,  $\text{CDCl}_3$ ) spectrum of rotaxane **13**· $\text{PF}_6^-$ . (b) HRMS ( $\text{ESI}^+$ ) spectrum of rotaxane **13**· $\text{PF}_6^-$ . Inset: Calculated (top) and experimental (bottom) isotopic distribution for the  $[\text{M}-\text{PF}_6]^+$  peak.

our system.  $[2]\text{rotaxane } 13\cdot\text{PF}_6^-$  was treated with  $\text{MgBr}_2$ , resulting in the controlled cleavage of its sulfonate unit. As no hydrogen bonding interactions are established between DB24C8 and non-protonated secondary amines, the addition of a base to deprotonate the dibenzylamine moiety led to a full release of the macrocycle from the cleaved thread (Fig. S5b in the  $\text{ESI}^\dagger$ ). After treatment with  $\text{Et}_3\text{N}$ , the compounds in the reaction mixture were separated by column chromatography. In this fashion we could isolate macrocycle **12** and a mixture of thread fragments **14/15** (1:1) in very good isolated yields (92% and 70% respectively) (Scheme 3b). Their identity was confirmed by NMR and MS techniques (see experimental procedure and Fig. S5, S61–S65 and S82–S85 in the  $\text{ESI}^\dagger$  for further details). The isolation of these compounds confirms the cleavage in a selective and controlled manner of the sulfonate moiety, supporting the release of the macrocycle through the opposite side of its entrance and the proposed operation mechanism.

### *In situ* operation

Having demonstrated that the transportation can be accomplished stepwise, our final goal was the *in situ* unidirectional transport of DB24C8 (**12**). For this purpose, we performed the sequence of reactions of the previous stepwise operation in  $\text{CDCl}_3$  and monitored them by HRMS and  $^1\text{H}$  NMR spectroscopy.

The first step was the assembly of a pseudorotaxane between DB24C8 (**12**) and thread precursor **10**· $\text{PF}_6^-$ , with an



unstoppered vinyl sulfone group on one end and a bulky sulfonate stopper on the opposite one. Therefore, by stirring both compounds in  $\text{CDCl}_3$  under the concentration and stoichiometry conditions discussed for the rotaxane synthesis, the generation of the pseudorotaxane was achieved. This was confirmed by the analysis of the chemical shift and integration of the diagnostic signals (*e.g.* those of  $\text{H}_a$ ,  $\text{H}_b$ ,  $\text{H}_c$  or  $\text{H}_1$ ) in the

$^1\text{H}$  NMR spectrum. These signals displayed chemical shifts and integration similar to those already discussed for the step-wise operation that can be associated with the establishment of hydrogen bond interactions between the crown ether and the ammonium unit (Fig. 4a-c). As previously observed, only one set of signals was observed for  $\mathbf{10}\text{-PF}_6^-$ , supporting a high degree of complexation with the concentration of free  $\mathbf{10}\text{-PF}_6^-$

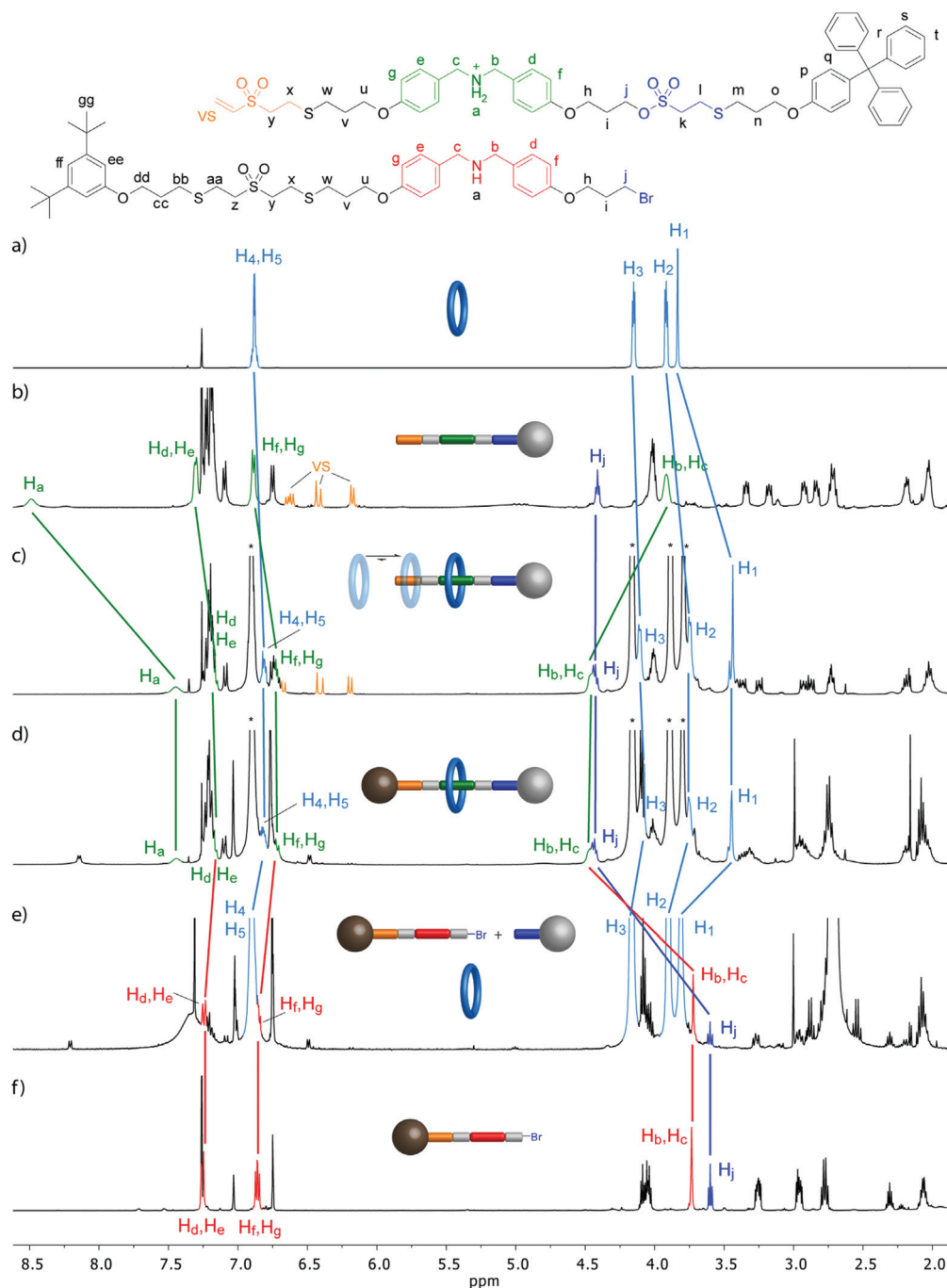


**Fig. 4** *In situ* unidirectional transport experiment of macrocycle **12**.  $^1\text{H}$  NMR ( $\text{CDCl}_3$ ) spectra of: (a) Macrocycle **12** (500 MHz). (b) Thread precursor **10**- $\text{PF}_6^-$  (500 MHz). (c) Mixture of **10**- $\text{PF}_6^-$  (21 mM) and **12** (5 equiv.) after stirring for 72 h (400 MHz). (d) Mixture c 96 h after the addition of stopper **11** and  $\text{DMAP}_{(\text{cat})}$  (signals at 8.1–8.2 ppm, 6.5 ppm and 3.0 ppm) (400 MHz). (e) Mixture d stirred for 48 h in the presence of  $\text{MgBr}_2$  and for additional 60 min after the addition of  $\text{Et}_3\text{N}$  (400 MHz). (f) Compound **14** (500 MHz). The signals marked with an asterisk correspond to the excess of DB24C8.



below the NMR detection limit. The pseudorotaxane was also detected by HRMS. Thus, the spectra of the mixture of **12** and  $10\cdot\text{PF}_6^-$  showed a peak ( $m/z = 1428.5527$ ), which matched the threaded species (Fig. S10 and S11†).<sup>30</sup>

Subsequent addition of thiol stopper **11** and a catalytic amount of DMAP as catalyst for the MAVS reaction between the thiol and the vinyl sulfone moieties afforded rotaxane  $13\cdot\text{PF}_6^-$ . As shown in Fig. 4d, the chemical shifts of the key signals remained essentially unaltered respect to the pseudorotaxane and were comparable to those of pure rotaxane  $13\cdot\text{PF}_6^-$  (Fig. 4d).<sup>31</sup> Moreover, the existence of rotaxane  $13\cdot\text{PF}_6^-$  was confirmed by HRMS since we detected the peak corresponding to its exact mass ( $m/z = 1708.7354$  for  $[\text{M}-\text{PF}_6^-]^+$ ) (Fig. S13 and S14†), which displayed an isotopic distribution that nicely matched the calculated one. In this way, the threading of the macrocycle through the unstoppered side of the thread and its capture by capping was achieved, completing the first part of the directional transport.

To finish the operation and release the macrocycle through the opposite side of the thread we performed the cleavage of the bulky sulfonate group of rotaxane  $13\cdot\text{PF}_6^-$  with  $\text{MgBr}_2$ . Positive-mode HRMS allowed the detection of a new signal belonging to the pseudorotaxane formed by macrocycle **12** and cleaved axle  $14\text{-H}^+\cdot\text{PF}_6^-$  ( $m/z: 1270.5002$   $[\text{M}-\text{PF}_6^-]^+$ ) (Fig. S16 and S17†).<sup>30</sup> Moreover, in negative mode, a signal corresponding to the sulfonate cleaved stopper **15** ( $m/z: 517.1504$   $[\text{M}]^-$ ) was also present (Fig. S18 and S19†). Lastly, after the addition of  $\text{Et}_3\text{N}$ , the  $^1\text{H}$  NMR spectrum showed the appearance of a triplet at  $\delta = 3.60$  ppm, which matches a  $\text{CH}_2\text{-Br}$  bond newly created, thus, corresponding to  $\text{H}_j$ . In addition, those of DB24C8 (**12**) shifted back to their original position (Fig. 4e). These results confirm the second part of the operation, in which the negligible interaction between crown ethers and non-protonated secondary amines promotes the macrocycle to be released from the thread through the opposite side of its entrance by cleavage of the sulfonate group, initially stoppered.

Therefore, the *in situ* unidirectional transport of DB24C8 in a [2]rotaxane by a combination of click MAVS reactions and the CAD chemistry of the vinyl sulfonate group is demonstrated.

## Conclusions

In summary, we have described the irreversible unidirectional transportation of a DB24C8 macrocycle along a dibenzylamine/ammonium axle, through a [2]rotaxane, exploiting the chemistry of the vinyl sulfone and the vinyl sulfonate groups. This system is based on a pH- and chemically-driven flashing ratchet mechanism. Indeed, initially, the macrocycle enters by the non-stoppered vinyl sulfone side of the molecule and *via* a thia-Michael addition of a thiol stopper to the latter, the rotaxane is capped. Subsequently, the MIM is cleaved through a nucleophilic attack on the sulfonate moiety derived from a vinyl sulfonate group on the opposite side and, finally, after addition of base, the macrocycle is liberated through the oppo-

site side to its entrance, achieving the unidirectional transportation. During the operation, the efficiency of the click MAVS chemistry and the CAD chemistry of the vinyl sulfonate group has again been demonstrated. As result, the operation of the system has also been demonstrated *in situ*.

Thus, the CAD chemistry of the vinyl sulfonate group is an efficient tool for the development of cleavable rotaxanes. Moreover, since it is possible to control the unidirectional translational movement of a ring through a rotaxane using a combination of the MAVS and CAD chemistries, the latter could be interesting potential tools for the development of future advanced delivery systems.

## Author contributions

A.H.G.D.: Investigation, formal analysis, validation, writing-original draft. P.G.-C.: Investigation, formal analysis, validation. A.G. C.: Conceptualization, funding acquisition, supervision. F.S.-G.: Funding acquisition, methodology, supervision. V.B.: Conceptualization, funding acquisition, formal analysis, methodology, supervision, project administration, writing-original draft.

## Conflicts of interest

There are no conflicts to declare.

## Acknowledgements

This work has been financially supported by FEDER(EDRF)/Junta de Andalucía-Consejería de Transformación Económica, Industria, Conocimiento y Universidades (P18-FR-2877), grant PID2020-112906GA-I00 funded by MCIN/AIE (/10.13039/501100011033) and Ministerio de Economía y Competitividad (MINECO, Spain) (CTQ2014-55474-C2-2-R and CTQ2017-86125-P, co-financed by FEDER funds). Funding for open access APCs provided by Universidad de Granada through a Paid by Read & Publish agreement with RSC.

## Notes and references

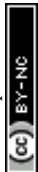
- 1 C. J. Bruns and J. F. Stoddart, *The Fundamentals of Making Mechanical Bonds*, John Wiley & Sons, Hoboken, 2016.
- 2 M. Xue, Y. Yang, X. Chi, X. Yan and F. Huang, Development of Pseudorotaxanes and Rotaxanes: From Synthesis to Stimuli-Responsive Motions to Applications, *Chem. Rev.*, 2015, **115**, 7398–7501.
- 3 (a) N. H. Evans and P. D. Beer, Progress in the synthesis and exploitation of catenanes since the Millennium, *Chem. Soc. Rev.*, 2014, **43**, 4658–4683; (b) G. Gil-Ramírez, D. A. Leigh and A. J. Stephens, Catenanes: Fifty Years of Molecular Links, *Angew. Chem., Int. Ed.*, 2015, **54**, 6110–6150.
- 4 (a) S. Erbas-Cakmak, D. A. Leigh, C. T. McTernan and A. L. Nussbaumer, Artificial Molecular Machines, *Chem.*



- Rev.*, 2015, **115**, 10081–10206; (b) L. Zhang, V. Marcos and D. A. Leigh, Molecular machines with bio-inspired mechanisms, *Proc. Natl. Acad. Sci. U. S. A.*, 2018, **115**, 9397–9404; (c) A. W. Heard and S. M. Goldup, Simplicity in the Design, Operation, and Applications of Mechanically Interlocked Molecular Machines, *ACS Cent. Sci.*, 2020, **6**, 117–128; (d) I. Aprahamian, The Future of Molecular Machines, *ACS Cent. Sci.*, 2020, **6**, 347–358.
- 5 (a) T. D. Nguyen, H.-R. Tseng, P. C. Celestre, A. H. Flood, Y. Liu, J. F. Stoddart and J. I. Zink, A reversible molecular valve, *Proc. Natl. Acad. Sci. U. S. A.*, 2005, **102**, 10029–10034; (b) K. Patel, S. Angelos, W. R. Dichtel, A. Coskun, Y.-W. Yang, J. I. Zink and J. F. Stoddart, Enzyme-Responsive Snap-Top Covered Silica Nanocontainers, *J. Am. Chem. Soc.*, 2008, **130**, 2382–2383; (c) A. Martinez-Cuezva, S. Valero-Moya, M. Alajarin and J. Berná, Light-responsive peptide [2]rotaxanes as gatekeepers of mechanised nanocontainers, *Chem. Commun.*, 2015, **51**, 14501–14504.
- 6 (a) Y. Liu, A. H. Flood, P. A. Bonvallet, S. A. Vignon, B. H. Northrop, H.-R. Tseng, J. O. Jeppesen, T. J. Huang, B. Brough, M. Baller, S. Magonov, S. D. Solares, W. A. Goddard, C.-M. Ho and J. F. Stoddart, Linear Artificial Molecular Muscles, *J. Am. Chem. Soc.*, 2005, **127**, 9745–9759; (b) J. Berná, D. A. Leigh, M. Lubomska, S. M. Mendoza, E. M. Pérez, P. Rudolf, G. Teobaldi and F. Zerbetto, Macroscopic transport by synthetic molecular machines, *Nat. Mater.*, 2005, **4**, 704–710; (c) A. Goujon, T. Lang, G. Mariani, E. Moulin, G. Fuks, J. Raya, E. Buhler and N. Giuseppone, Bistable [c2] Daisy Chain Rotaxanes as Reversible Muscle-like Actuators in Mechanically Active Gels, *J. Am. Chem. Soc.*, 2017, **139**, 14825–14828; (d) S. Ikejiri, Y. Takashima, M. Osaki, H. Yamaguchi and A. Harada, Solvent-Free Photoresponsive Artificial Muscles Rapidly Driven by Molecular Machines, *J. Am. Chem. Soc.*, 2018, **140**, 17308–17315.
- 7 (a) G. Bottari, D. A. Leigh and E. M. Pérez, Chiroptical Switching in a Bistable Molecular Shuttle, *J. Am. Chem. Soc.*, 2003, **125**, 13360–13361; (b) Q.-C. Wang, D.-H. Qu, J. Ren, K. Chen and H. Tian, A Lockable Light-Driven Molecular Shuttle with a Fluorescent Signal, *Angew. Chem., Int. Ed.*, 2004, **43**, 2661–2665; (c) D. A. Leigh, M. Á. F. Morales, E. M. Pérez, J. K. Y. Wong, C. G. Saiz, A. M. Z. Slawin, A. J. Carmichael, D. M. Haddleton, A. M. Brouwer, W. J. Buma, G. W. H. Wurpel, S. León and F. Zerbetto, Patterning through Controlled Submolecular Motion: Rotaxane-Based Switches and Logic Gates that Function in Solution and Polymer Films, *Angew. Chem., Int. Ed.*, 2005, **44**, 3062–3067; (d) H. Onagi and J. Rebek, Jr., Fluorescence resonance energy transfer across a mechanical bond of a rotaxane, *Chem. Commun.*, 2005, 4604–4606; (e) Z.-Q. Cao, Z.-L. Luan, Q. Zhang, R.-R. Gu, J. Ren and D.-H. Qu, An acid/base responsive side-chain polyrotaxane system with a fluorescent signal, *Polym. Chem.*, 2016, **7**, 1866–1870; (f) Y. Sagara, M. Karman, A. Seki, M. Pannipara, N. Tamaoki and C. Weder, Rotaxane-Based Mechanophores Enable Polymers with Mechanically Switchable White Photoluminescence, *ACS Cent. Sci.*, 2019, **5**, 874–881; (g) A. H. G. David, R. Casares, J. M. Cuerva, A. G. Campaña and V. Blanco, A [2]Rotaxane-Based Circularly Polarized Luminescence Switch, *J. Am. Chem. Soc.*, 2019, **141**, 18064–18074; (h) W.-J. Li, Q. Gu, X.-Q. Wang, D.-Y. Zhang, Y.-T. Wang, X. He, W. Wang and H.-B. Yang, AIE-Active Chiral [3]Rotaxanes with Switchable Circularly Polarized Luminescence, *Angew. Chem., Int. Ed.*, 2021, **60**, 9507–9515.
- 8 (a) V. Blanco, A. Carlone, K. D. Hänni, D. A. Leigh and B. Lewandowski, A Rotaxane-Based Switchable Organocatalyst, *Angew. Chem., Int. Ed.*, 2012, **51**, 5166–5169; (b) V. Blanco, D. A. Leigh, V. Marcos, J. A. Morales-Serna and A. L. Nussbaumer, A Switchable [2]Rotaxane Asymmetric Organocatalyst That Utilizes an Acyclic Chiral Secondary Amine, *J. Am. Chem. Soc.*, 2014, **136**, 4905–4908; (c) A. Martinez-Cuezva, A. Saura-Sanmartin, T. Nicolas-Garcia, C. Navarro, R.-A. Orenes, M. Alajarin and J. Berna, Photoswitchable interlocked thiodiglycolamide as a cocatalyst of a chalcogeno-Baylis–Hillman reaction, *Chem. Sci.*, 2017, **8**, 3775–3780; (d) C. Biagini, S. D. P. Fielden, D. A. Leigh, F. Schaufelberger, S. Di Stefano and D. Thomas, Dissipative Catalysis with a Molecular Machine, *Angew. Chem., Int. Ed.*, 2019, **58**, 9876–9880; (e) M. Calles, J. Puigerver, D. A. Alonso, M. Alajarin, A. Martinez-Cuezva and J. Berna, Enhancing the selectivity of prolinamide organocatalysts using the mechanical bond in [2]rotaxanes, *Chem. Sci.*, 2020, **11**, 3629–3635.
- 9 (a) C. P. Collier, E. W. Wong, M. Belohradsky, F. M. Raymo, J. F. Stoddart, P. J. Kuekes, R. S. Williams and J. R. Heath, Electronically Configurable Molecular-Based Logic Gates, *Science*, 1999, **285**, 391–394; (b) J. E. Green, J. W. Choi, A. Boukai, Y. Bunimovich, E. Johnston-Halperin, E. DeIonno, Y. Luo, B. A. Sheriff, K. Xu, Y. S. Shin, H.-R. Tseng, J. F. Stoddart and J. R. Heath, A 160-kilobit molecular electronic memory patterned at 1011 bits per square centimetre, *Nature*, 2007, **445**, 414–417.
- 10 (a) B. Lewandowski, G. De Bo, J. W. Ward, M. Pappmeyer, S. Kuschel, M. J. Aldegunde, P. M. E. Gramlich, D. Heckmann, S. M. Goldup, D. M. D'Souza, A. E. Fernandes and D. A. Leigh, Sequence-Specific Peptide Synthesis by an Artificial Small-Molecule Machine, *Science*, 2013, **339**, 189–193; (b) G. De Bo, M. A. Y. Gall, M. O. Kitching, S. Kuschel, D. A. Leigh, D. J. Tetlow and J. W. Ward, Sequence-Specific  $\beta$ -Peptide Synthesis by a Rotaxane-Based Molecular Machine, *J. Am. Chem. Soc.*, 2017, **139**, 10875–10879; (c) C. T. McTernan, G. De Bo and D. A. Leigh, A Track-Based Molecular Synthesizer that Builds a Single-Sequence Oligomer through Iterative Carbon-Carbon Bond Formation, *Chem*, 2020, **6**, 2964–2973; (d) J. Echavarren, M. A. Y. Gall, A. Haertsch, D. A. Leigh, J. T. J. Spence, D. J. Tetlow and C. Tian, Sequence-selective decapeptide synthesis by the parallel operation of two artificial molecular machines, *J. Am. Chem. Soc.*, 2021, **143**, 5158–5165.
- 11 J. D. Badjić, V. Balzani, A. Credi, S. Silvi and J. F. Stoddart, A Molecular Elevator, *Science*, 2004, **303**, 1845–1849.



- 12 (a) C. J. Bruns and J. F. Stoddart, Rotaxane-Based Molecular Muscles, *Acc. Chem. Res.*, 2014, **47**, 2186–2199; (b) A. Goujon, E. Moulin, G. Fuks and N. Giuseppone, [c2] Daisy Chain Rotaxanes as Molecular Muscles, *CCS Chem.*, 2019, **1**, 83–96.
- 13 (a) S. Kassem, T. van Leeuwen, A. S. Lubbe, M. R. Wilson, B. L. Feringa and D. A. Leigh, Artificial molecular motors, *Chem. Soc. Rev.*, 2017, **46**, 2592–2621; (b) M. Baroncini, S. Silvi and A. Credi, Photo- and Redox-Driven Artificial Molecular Motors, *Chem. Rev.*, 2020, **120**, 200–268; (c) Y. Qiu, Y. Feng, Q.-H. Guo, R. D. Astumian and J. F. Stoddart, Pumps through the Ages, *Chem*, 2020, **6**, 1954–1979; (d) Y. Feng, M. Ovalle, J. S. W. Seale, C. K. Lee, D. J. Kim, R. D. Astumian and J. F. Stoddart, Molecular Pumps and Motors, *J. Am. Chem. Soc.*, 2021, **143**, 5569–5591; (e) S. Corra, L. Casimiro, M. Baroncini, J. Groppi, M. La Rosa, M. Tranfić Bakić, S. Silvi and A. Credi, Artificial Supramolecular Pumps Powered by Light, *Chem. – Eur. J.*, 2021, **27**, 11076–11083.
- 14 (a) M. N. Chatterjee, E. R. Kay and D. A. Leigh, Beyond Switches: Ratcheting a Particle Energetically Uphill with a Compartmentalized Molecular Machine, *J. Am. Chem. Soc.*, 2006, **128**, 4058–4073; (b) V. Serrelli, C.-F. Lee, E. R. Kay and D. A. Leigh, A molecular information ratchet, *Nature*, 2007, **445**, 523–527; (c) M. Alvarez-Pérez, S. M. Goldup, D. A. Leigh and A. M. Z. Slawin, A Chemically-Driven Molecular Information Ratchet, *J. Am. Chem. Soc.*, 2008, **130**, 1836–1838.
- 15 (a) D. A. Leigh, J. K. Y. Wong, F. Dehez and F. Zerbetto, Unidirectional rotation in a mechanically interlocked molecular rotor, *Nature*, 2003, **424**, 174–179; (b) J. V. Hernández, E. R. Kay and D. A. Leigh, A Reversible Synthetic Rotary Molecular Motor, *Science*, 2004, **306**, 1532–1537; (c) M. Baroncini, S. Silvi, M. Venturi and A. Credi, Photoactivated Directionally Controlled Transit of a Non-Symmetric Molecular Axle Through a Macrocyclic, *Angew. Chem., Int. Ed.*, 2012, **51**, 4223–4226; (d) G. Ragazzon, M. Baroncini, S. Silvi, M. Venturi and A. Credi, Light-powered autonomous and directional molecular motion of a dissipative self-assembling system, *Nat. Nanotechnol.*, 2015, **10**, 70–75; (e) M. Canton, J. Groppi, L. Casimiro, S. Corra, M. Baroncini, S. Silvi and A. Credi, Second-Generation Light-Fueled Supramolecular Pump, *J. Am. Chem. Soc.*, 2021, **143**, 10890–10894.
- 16 (a) H. Li, C. Cheng, P. R. McGonigal, A. C. Fahrenbach, M. Frasconi, W.-G. Liu, Z. Zhu, Y. Zhao, C. Ke, J. Lei, R. M. Young, S. M. Dyar, D. T. Co, Y.-W. Yang, Y. Y. Botros, W. A. Goddard III, M. R. Wasielewski, R. D. Astumian and J. F. Stoddart, Relative Unidirectional Translation in an Artificial Molecular Assembly Fueled by Light, *J. Am. Chem. Soc.*, 2013, **135**, 18609–18620; (b) C. Cheng, P. R. McGonigal, W.-G. Liu, H. Li, N. A. Vermeulen, C. Ke, M. Frasconi, C. L. Stern, W. A. Goddard III and J. F. Stoddart, Energetically Demanding Transport in a Supramolecular Assembly, *J. Am. Chem. Soc.*, 2014, **136**, 14702–14705; (c) C. Cheng, P. R. McGonigal, S. T. Schneebeli, H. Li, N. A. Vermeulen, C. Ke and J. F. Stoddart, An artificial molecular pump, *Nat. Nanotechnol.*, 2015, **10**, 547–553; (d) Y. Qiu, B. Song, C. Pezzato, D. Shen, W. Liu, L. Zhang, Y. Feng, Q.-H. Guo, K. Cai, W. Li, H. Chen, M. T. Nguyen, Y. Shi, C. Cheng, R. D. Astumian, X. Li and J. F. Stoddart, A precise polyrotaxane synthesizer, *Science*, 2020, **368**, 1247–1253; (e) L. Feng, Y. Qiu, Q.-H. Guo, Z. Chen, J. S. W. Seale, K. He, H. Wu, Y. Feng, O. K. Farha, R. D. Astumian and J. F. Stoddart, Active mechanisorption driven by pumping cassettes, *Science*, 2021, **374**, 1215–1221.
- 17 (a) M. R. Wilson, J. Solá, A. Carlone, S. M. Goldup, N. Lebrasseur and D. A. Leigh, An autonomous chemically fuelled small-molecule motor, *Nature*, 2016, **534**, 235–240; (b) S. Erbas-Cakmak, S. D. P. Fielden, U. Karaca, D. A. Leigh, C. T. McTernan, D. J. Tetlow and M. R. Wilson, Rotary and linear molecular motors driven by pulses of a chemical fuel, *Science*, 2017, **358**, 340–343; (c) S. Amano, S. D. P. Fielden and D. A. Leigh, A catalysis-driven artificial molecular pump, *Nature*, 2021, **594**, 529–534.
- 18 (a) C. Reuter, W. Wienand, G. M. Hübner, C. Seel and F. Vögtle, High-Yield Synthesis of Ester, Carbonate, and Acetal Rotaxanes by Anion Template Assistance and their Hydrolytic Dethreading, *Chem. – Eur. J.*, 1999, **5**, 2692–2697; (b) A. Fernandes, A. Viterisi, F. Coutrot, S. Potok, D. A. Leigh, V. Aucagne and S. Papot, Rotaxane-Based Propeptides: Protection and Enzymatic Release of a Bioactive Pentapeptide, *Angew. Chem., Int. Ed.*, 2009, **48**, 6443–6447; (c) R. Barat, T. Legigan, I. Tranoy-Opalinski, B. Renoux, E. Péraudeau, J. Clarhaut, P. Poinot, A. E. Fernandes, V. Aucagne, D. A. Leigh and S. Papot, A mechanically interlocked molecular system programmed for the delivery of an anticancer drug, *Chem. Sci.*, 2015, **6**, 2608–2613; (d) C. C. Slack, J. A. Finbloom, K. Jeong, C. J. Bruns, D. E. Wemmer, A. Pines and M. B. Francis, Rotaxane probes for protease detection by <sup>129</sup>Xe hyperCEST NMR, *Chem. Commun.*, 2017, **53**, 1076–1079; (e) S.-T. Tung, H.-T. Cheng, A. Inthasot, F.-C. Hsueh, T.-J. Gu, P.-C. Yan, C.-C. Lai and S.-H. Chiu, Interlocked Photo-degradable Macrocycles Allow One-Off Photo-triggerable Gelation of Organo- and Hydrogelators, *Chem. – Eur. J.*, 2018, **24**, 1522–1527; (f) M. Zhang and G. De Bo, Mechanical Susceptibility of a Rotaxane, *J. Am. Chem. Soc.*, 2019, **141**, 15879–15883.
- 19 Z. Meng, J.-F. Xiang and C.-F. Chen, Directional Molecular Transportation Based on a Catalytic Stopper-Leaving Rotaxane System, *J. Am. Chem. Soc.*, 2016, **138**, 5652–5658.
- 20 H.-Y. Zhou, Y. Han, Q. Shi and C.-F. Chen, Directional Transportation of a Helic[6]arene along a Nonsymmetric Molecular Axle, *J. Org. Chem.*, 2019, **84**, 5872–5876.
- 21 Q.-H. Guo, Y. Qiu, X. Kuang, J. Liang, Y. Feng, L. Zhang, Y. Jiao, D. Shen, R. D. Astumian and J. F. Stoddart, Artificial Molecular Pump Operating in Response to Electricity and Light, *J. Am. Chem. Soc.*, 2020, **142**, 14443–14449.
- 22 (a) B. A. Frankel, M. Bentley, R. G. Kruger and D. G. McCafferty, Vinyl Sulfones: Inhibitors of SrtA, a



- Transpeptidase Required for Cell Wall Protein Anchoring and Virulence in *Staphylococcus aureus*, *J. Am. Chem. Soc.*, 2004, **126**, 3404–3405; (b) S. Liu, B. Zhou, H. Yang, Y. He, Z.-X. Jiang, S. Kumar, L. Wu and Z.-Y. Zhang, Aryl Vinyl Sulfonates and Sulfones as Active Site-Directed and Mechanism-Based Probes for Protein Tyrosine Phosphatases, *J. Am. Chem. Soc.*, 2008, **130**, 8251–8260; (c) J. Morales-Sanfrutos, F. J. Lopez-Jaramillo, F. Hernandez-Mateo and F. Santoyo-Gonzalez, Vinyl Sulfone Bifunctional Tag Reagents for Single-Point Modification of Proteins, *J. Org. Chem.*, 2010, **75**, 4039–4047; (d) T. del Castillo, J. Marales-Sanfrutos, F. Santoyo-González, S. Magez, F. J. Lopez-Jaramillo and J. A. Garcia-Salcedo, Monovinyl Sulfone  $\beta$ -Cyclodextrin. A Flexible Drug Carrier System, *ChemMedChem*, 2014, **9**, 383–389; (e) S. Chatani, C. Wang, M. Podgórski and C. N. Bowman, Triple Shape Memory Materials Incorporating Two Distinct Polymer Networks Formed by Selective Thiol–Michael Addition Reactions, *Macromolecules*, 2014, **47**, 4949–4954; (f) F. M. Tomlin, U. I. M. Gerling-Driessen, Y.-C. Liu, R. A. Flynn, J. R. Vangala, C. S. Lentz, S. Clauder-Muenster, P. Jakob, W. F. Mueller, D. Ordoñez-Rueda, M. Paulsen, N. Matsui, D. Foley, A. Rafalko, T. Suzuki, M. Bogyo, L. M. Steinmetz, S. K. Radhakrishnan and C. R. Bertozzi, Inhibition of NGLY1 Inactivates the Transcription Factor Nrf1 and Potentiates Proteasome Inhibitor Cytotoxicity, *ACS Cent. Sci.*, 2017, **3**, 1143–1155; (g) J. Sinha, M. Podgórski, S. Huang and C. N. Bowman, Multifunctional monomers based on vinyl sulfonates and vinyl sulfonamides for crosslinking thiol–Michael polymerizations: monomer reactivity and mechanical behavior, *Chem. Commun.*, 2018, **54**, 3034–3037.
- 23 A. H. G. David, P. García-Cerezo, A. G. Campaña, F. Santoyo-González and V. Blanco, [2]Rotaxane End-Capping Synthesis by Click Michael-Type Addition to the Vinyl Sulfonyl Group, *Chem. – Eur. J.*, 2019, **25**, 6170–6179.
- 24 R. Bielski and Z. Witczak, Strategies for Coupling Molecular Units if Subsequent Decoupling Is Required, *Chem. Rev.*, 2013, **113**, 2205–2243.
- 25 C. M. Cruz, M. Ortega-Muñoz, F. J. López-Jaramillo, F. Hernández-Mateo, V. Blanco and F. Santoyo-González, Vinyl Sulfonates: A Click Function for Coupling-and-Decoupling Chemistry and their Applications, *Adv. Synth. Catal.*, 2016, **358**, 3394–3413.
- 26 P. R. Ashton, P. J. Campbell, E. J. T. Chrystal, P. T. Glink, S. Menzer, D. Philp, N. Spencer, J. F. Stoddart, P. A. Tasker and D. J. Williams, Dialkylammonium Ion/Crown Ether Complexes: The Forerunners of a New Family of Interlocked Molecules, *Angew. Chem., Int. Ed. Engl.*, 1995, **34**, 1865–1869.
- 27 It should be noted that the complexation process between DB24C8 and dibenzylammonium derivatives is slow on the NMR timescale. Therefore, by performing the operation with an excess of macrocycle, we also simplify the monitoring by NMR, especially during the *in situ* operation, avoiding the presence of an additional set of signals corresponding to the unbound  $10\text{-PF}_6^-$ . In addition, the excess of **12** also helps to improve the solubility of  $10\text{-PF}_6^-$  in  $\text{CDCl}_3$ , usually quite poor.
- 28 K. Nakazono, T. Oku and T. Takata, Synthesis of rotaxanes consisting of crown ether wheel and *sec*-ammonium axle under basic condition, *Tetrahedron Lett.*, 2007, **48**, 3409–3411.
- 29 P. Place, M. L. Roumestant and J. Gore, Reaction of magnesium halides with sulfonates, *Bull. Soc. Chim. Fr.*, 1976, 169–176.
- 30 During the analysis of the pseudorotaxanes assembled from DB24C8 (**12**) and  $10\text{-PF}_6^-$  or  $14\text{-H}^+\text{-PF}_6^-$ , peaks corresponding to the free ammonium salts (calculated *m/z*: 980.3358  $[\text{M-PF}_6^-]^+$  for  $10\text{-PF}_6^-$ ; 822.2895  $[\text{M-PF}_6^-]^+$  for  $14\text{-H}^+\text{-PF}_6^-$ ) can also be detected in some cases (e. g. Fig. S10†) depending on the experimental conditions, such as concentration or ionization potential. In fact, the dissociation of the pseudorotaxane is not surprising at low concentrations and in the presence of a hydrogen bonding competitive solvent as MeOH, conditions used in ESI mass spectrometry measurements.
- 31 Minor traces of an unknown by-product that seems to possess an alkene group with peaks in the region between 6.2 and 6.4 ppm can be in some cases detected by NMR spectroscopy.

